Poly(pyridinium salt)s with organic counterions derived from an aromatic diamine containing oxyethylene unit exhibiting amphotropic liquid-crystalline and photoluminescence properties

Pradip K. Bhowmik [a,*], Haesook Han [a], Alexi K. Nedeltchev [a], Hari D. Mandal [b], Jose A. Jimenez-Hernandez [b], Patrick M. McGannon [b]

[a] Department of Chemistry, University of Nevada at Las Vegas, 4505 Maryland Parkway, Box 454003, Las Vegas, NV 89154, USA
[b] Department of Biology and Chemistry, Texas A&M International University, 5201 University Boulevard, Laredo, TX 78041, USA

ARTICLE INFO

ABSTRACT

Several poly(pyridinium salt)s containing various organic counterions and oxyethylene unit in their backbones were synthesized by either the ring-transmutation polymerization reaction of 4,4'-(1,4-phenylene)bis(2,6-diphenylpyrylium tosylate) with 1,2-bis(4-aminophenoxy)ethane on heating in dimethyl sulfoxide or the metathesis reaction of the tosylate polymer with the corresponding lithium or sodium salts in acetonitrile. Their chemical structures were determined by ^{1}H and ^{13}C NMR spectroscopy, and elemental analyses. Their number-average molecular weights and polydispersity indices were in the range of 59,000–63,000 and 1.41–1.65, respectively, as determined by gel permeation chromatography. They were characterized for their thermotropic and lyotropic liquid-crystalline properties by using differential scanning calorimetry and polarizing optical microscopy. Since these polymers exhibited liquid-crystalline phase both in the melt and in solutions, they belong to an amphotropic class of ionic polymers. Their light-emitting properties both in polar organic solvents and in films cast from methanol and acetonitrile were also studied by using spectrofluorometry.

© 2009 Elsevier Ltd. All rights reserved.

1. Introduction

Poly(pyridinium salt)s are an important class of macromolecules that contain ionic groups in their backbones, since they are suitable polymers for building up multilayer assemblies. On the one hand, these polymers containing tosylate or triflimide counterions, prepared from phenylated bis(pyrylium salt)s and aromatic diamines such as benzidine, 4,4'-oxydianiline and 2,6-diaminoanthracene, exhibited lyotropic liquid-crystalline phase (LC) in various polar organic solvents such as dimethyl sulfoxide (DMSO), acetonitrile, and methanol at various critical concentrations (C^*) depending on the chemical structures of aromatic diamines used. They also exhibited photoluminescence properties both in solutions and in the solid state [1,2]. Similarly, polymers containing tosylate as counterion, prepared by reacting 2-naphthylated bis(pyrylium salt)s with both 4,4'-oxydianiline and 4,4'-methylenedianiline, showed lyotropic LC phase in methanol and DMSO at varying C^* values. They also showed photoluminescence properties in these solvents [3]. Polymers containing 2-naphthalenesulfonate as

counterion, prepared by reacting 4,4'-(1,4-phenylene)bis(2,6-diphenylpyrylium 2-naphthalenesulfonate) with both 4,4'-oxydianiline and 4,4'-methylenedianiline, also showed lyotropic LC phase in these polar solvents at varying C^* values. They also showed photoluminescence properties in these solvents [4]. On the other hand, ionic polymers containing tosylate or triflimide counterions, prepared from phenylated bis(pyrylium salt)s and 1,9-diaminononane or 1,12-diaminododecane, exhibited both thermotropic LC and photoluminescence properties [5,6]. Additionally, ionic polymers containing tosylate or triflimide counterions, prepared from phenylated bis(pyrylium salt)s and oxyalkylene diamines, showed amphotropic LC and light-emitting properties [7]. In this article, we describe the synthesis of a series of poly(pyridinium salt)s containing four organic counterions and one oxyethylene unit in their backbones by ring-transmutation and metathesis reactions [1], and the characterization of their both thermotropic and lyotropic LC properties in various organic solvents by using several experimental techniques. Their light-emitting properties in various organic solvents and in the solid state were also examined by using photoluminescence spectrometry. The general structures and designations of these ionic polymers, **I**, which were used in this study, are shown in Scheme 1.
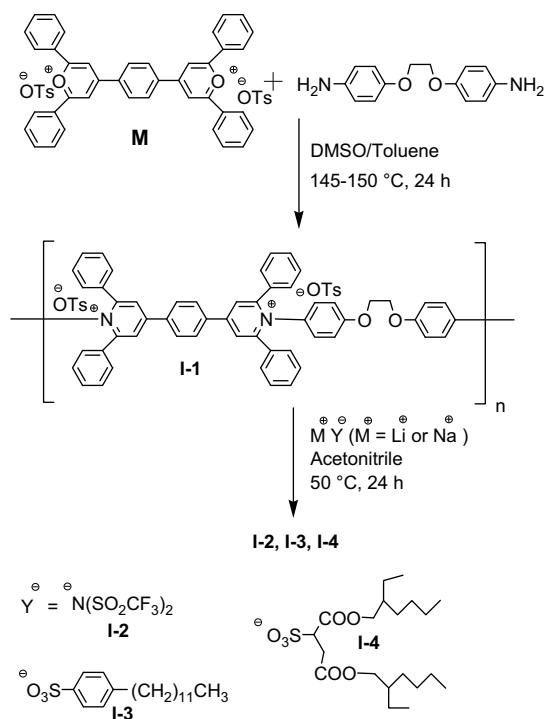
Scheme 1.

2. Experimental section

2.1. Monomer synthesis

The 4,4′-(1,4-phenylene)bis(2,6-diphenylpyrylium)ditosylate, **M**, was synthesized according to the known procedure [1] as shown in Scheme 2. 1,2-Bis(4-aminophenoxy)ethane was synthesized also according to the known procedure with a yield of 88% [8]. Anal. Calcd for $C_{14}H_{16}N_2O_2$ (244.29): C, 68.83; H, 6.60; N, 11.47. Found: C, 68.80; H, 7.00; N,11.74. It showed a sharp melting endotherm ($\Delta H = 48.4$ kJ/mol) at peak maximum of 179 °C in the first heating cycle of its DSC thermogram, obtained at a heating rate of 10 °C/min. It also showed essentially similar melting endotherm with identical enthalpy change in the second heating cycle (mp 178–179 °C) [8]. However, there were additionally a small exotherm and a small

endotherm in the low-temperature region prior to the melting endotherm. The lithium triflimide, sodium dodecylbenzenesulfonate (NaDBS), and sodium docusate (dioctylsulfosuccinate) were also purchased from Sigma–Aldrich Chemical Company and used them without further purification for the metathesis reaction.

2.2. Polymer synthesis

2.2.1. Synthesis of polymer I-1

The bis(pyrylium salt) **M** was polymerized with 1,2-bis(4-aminophenoxy)ethane by ring-transmutation polymerization reaction [1] to yield polymer **I-1** that was carried out on heating in DMSO as shown in Scheme 1. Anal. Calcd for $C_{68}H_{54}N_2O_8S_2$ (1091.32) (**I-1**): C, 74.84; H, 4.99; N, 2.57; S, 5.88. Found: C, 72.13; H, 5.39; N, 2.45; S, 5.90.

2.2.2. Synthesis of polymers I-2–I-4

All of them were prepared by the metathesis reaction of polymer **I-1** with the corresponding salts in a common organic solvent, such as acetonitrile [1]. Anal. Calcd for $C_{58}H_{40}N_4O_{11}F_{12}S_2$ (1309.21) (**I-2**): C, 53.21; H, 3.08; N, 4.28; S, 9.80. Found: C, 51.57; H, 2.99; N, 4.48; S, 9.62. Anal. Calcd for $C_{90}H_{98}N_2O_8S_2$ (1399.92) (**I-3**): C, 77.22; H, 7.06; N, 2.00; S, 4.58. Found: C, 75.39; H, 6.70; N, 2.28; S, 3.80. Anal. Calcd for $C_{94}H_{114}N_2O_{16}S_2$ (1592.09) (**I-4**): C, 70.92; H, 7.22; N, 1.76; S, 4.03. Found: C, 70.80; H, 6.91; N, 2.15; S, 4.41.

2.3. Polymer characterization

The ^1H and ^{13}C NMR spectra of polymers **I-1**–**I-4** were recorded with a VNMR 400 spectrometer with three RF channels operating at 400 and 100 MHz, respectively, in d_6-DMSO using TMS as an internal standard. Gel permeation chromatography (GPC) was performed for the synthesized polymers in DMSO at 40 °C with a flow rate 1.0 mL/min with a Waters 515 pump together with a Viscotek Model 301 Triple Detector Array that combines a laser refractometer, a differential viscometer, and a RALLS (right angle laser light scattering)/LALLS (low angle laser light scattering) at 7° detectors in a single instrument with fixed inter-detector volumes and temperature control to 80 °C. Although conventional chromatographic calibrations are not required for this type of GPC instrument, the pullulan standards of P-10 and P-50 from Polymer Standards Services USA, Inc. were used for the instrument calibration. Separations were accomplished using ViscoGel I-MBHMW-3078 columns from
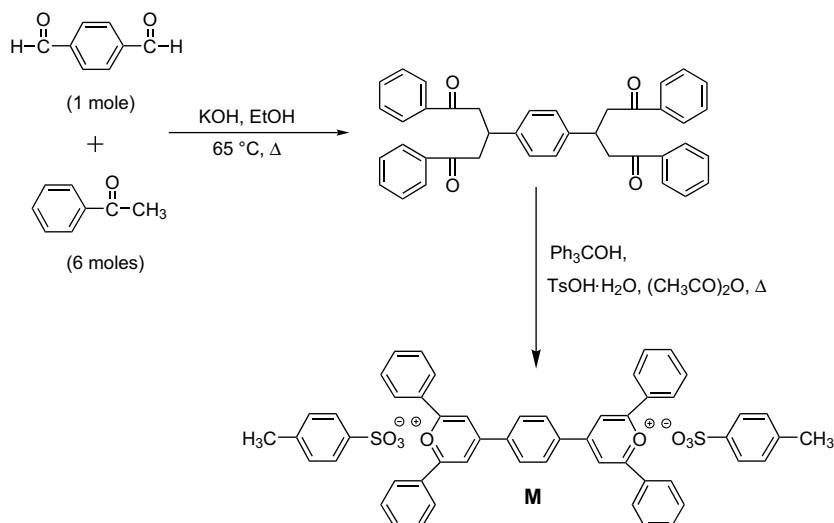
Scheme 2.

Table 1
GPC data for ionic polymers **I-1**–**I-4**.

Polymer	IV (dL/g)	M_n	M_w	M_w/M_n	dn/dc (ml/g)	R_g (nm)	α	K
I-1	0.59	59,498	84,219	1.42	0.0790	19.60	0.85	4.30×10^{-5}
I-2	0.57	59,756	93,535	1.57	0.0790	26.40	0.70	2.06×10^{-4}
I-3	0.47	63,375	104,820	1.65	0.0650	17.77	0.75	9.08×10^{-5}
I-4	1.22	58,930	83,214	1.41	0.1200	20.89	0.92	3.89×10^{-5}

Viscotek. A 100 μL of 0.2 wt% of polymer in DMSO containing 0.01 M LiBr was injected into the columns. Data analyses were performed using Viscotek TriSEC software. Phase transition temperatures were measured with a TA 2100 differential scanning calorimeter (DSC) under nitrogen flow at heating and cooling rates of 10 °C/min. The temperature axis of the DSC thermogram was calibrated before use with the reference standard of high-purity indium and tin. Polymers usually weighing 8–10 mg were used for these analyses. The thermogravimetric analysis (TGA) was performed with a TA 2100 instrument at a heating rate of 10 °C/min in nitrogen. Both thermotropic and lyotropic LC properties of the polymers **I-1**–**I-4** were studied using a polarized optical microscopy (POM, Nikon, Model Labophot 2) equipped with crossed polarizer and a hot stage. Samples of these ionene polymers for lyotropic properties were made by dissolving known amounts of polymers into known amounts of specific solvents. The UV–vis absorption spectra of polymers **I-1**–**I-4** in spectrograde organic solvents were recorded with a Varian Cray 3 Bio UV–vis spectrophotometer at ambient temperature. Their photoluminescence spectra in solutions and solvent-cast thin films were recorded with a Perkin–Elmer LS 55 luminescence spectrometer with a xenon lamp light source.

3. Results and discussion

3.1. Chemical structures

The ^{1}H and ^{13}C NMR spectra of polymer **I-1** (Fig. S1) along with its elemental analysis data were consistent with its chemical structure. Additionally, its ^{13}C NMR spectrum contained only aromatic carbon signals of phenylated pyridinium moieties. The carbonyl resonance at ca. 187 ppm [9], which is attributable to a vinylogous amide, was not detected in this polymer suggesting that the ring-transmutation polymerization reaction proceeded to completion under the experimental conditions used. The proton signals of vinylogous amide and amino end groups were also not detected in its ^{1}H NMR spectrum suggesting that it was of moderate molecular weight polymer. The ^{1}H and ^{13}C NMR spectra (Figs. S2–S4) and elemental analysis data of polymers **I-2**–**I-4** also confirmed their chemical structures. The absence of tosylate proton signals in polymers **I-2** and **I-4** (Figs. S2 and S4) suggested that the exchange of tosylate ions in polymer **I-1** with triflimide and docusate ions, respectively, was effective in the metathesis reaction under the experimental protocols used for these polymers. The complete absence of aromatic protons as well as methyl proton signals of tosylate ions in polymer **I-3** and appearance of aromatic protons at slightly different chemical shifts and of different shapes when compared with tosylate aromatic proton signals in polymer **I-1** as well as aliphatic proton signals at different chemical shifts of DBS (Fig. S3) also suggested that metathesis reaction for the preparation of this polymer from polymer **I-1** proceeded smoothly as expected.

3.2. Gel permeation chromatography of ionic polymers

In GPC measurements of ionic polymers **I-1**–**I-4** by Viscotek triple-detector SEC system, the inter-detector signals, that is, refractometer, viscometer, and RALLS/LALLS signals are overall excellent in all cases

(not shown). The data including radius of gyration, and Mark–Houwink α and K values from these studies of synthesized polymers are compiled in Table 1. These data indicated that they had intrinsic viscosities in the range of 0.59–1.22 dL/g, number-average molecular weights (M_n) in the range of 59,000–63,000, weight-average molecular weights (M_w) in the range of 83,000–105,000 and polydispersity indices in the range of 1.41–1.65. As expected, the molecular weights and polydispersity indices of these polymers are essentially in the similar range, since **I-2**–**I-4** were synthesized by the metathesis reactions of polymer **I-1** with the corresponding salts in an organic solvent [1]. Thus, it is quite reasonable to assume that all of these ionic polymers had sufficiently high molecular weights for a meaningful comparison of their both thermotropic and lyotropic liquid-crystalline properties (vide infra). In other words, the thermal, solution, optical and other physical properties can presumably be compared without concerns for the secondary effects of molecular weights on these properties.

3.3. Thermotropic liquid-crystalline properties

Fig. 1a shows the DSC thermograms of polymer **I-1** obtained at heating and cooling rates of 10 °C/min in nitrogen. In the first heating cycle, it exhibited two broad endotherms. The low-temperature endotherm was related to the loss of residual solvent in the polymer and the high-temperature endotherm was related to the crystal-to-LC transition (T_m) at ca. 251 °C. In the second heating cycle, it showed a distinct T_g at 216 °C and but no melting endotherm. In each of the cooling cycles, there was a single T_g. On melting it formed a very viscous melt that hindered the development of identifiable LC texture. However, it developed crescent-shaped, birefringent specs (Fig. 2a) on annealing at 290 °C overnight indicating its LC texture when examined under the crossed polarizers of a microscope. This LC texture persisted up to its decomposition temperature at 337 °C, as determined by TGA at a heating rate of 10 °C/min in nitrogen. In other words, its T_i was not detected in the DSC thermograms and also could not be determined with heating the polymer on the hot stage of POM studies. In the first heating cycle of polymer **I-2**, there were two broad endotherms (Fig. 1b). The low-temperature endotherm was also related to the loss of residual solvent in this polymer. The high-temperature endotherm was related to LC-to-isotropic liquid transition (T_i) at 365 °C as verified with POM studies, the temperature at which the disappearance of highly birefringent texture occurred. In the second heating cycle, it showed a distinct T_g at 168 °C and exceedingly broad endotherm. However, with heating to a temperature of ca. 52 °C higher than the T_g, it formed a highly birefringent melt suggesting its LC texture (Fig. 2b). The absence of T_m in the DSC thermogram was related to the low enthalpy of melting, which was beyond the detection limit of DSC instrument used. Polymer **I-2** had not only a broad temperature range LC phase of ca. 145 °C but also a high thermal stability of 438 °C, as determined by TGA (Fig. 3). In fact, it had the highest thermal stability and polymer **I-4** had the lowest thermal stability of 300 °C (Fig. 3) among all the polymers in this series, as expected. All of these results are consistent with those reported earlier in the literature [5–7]. The features of DSC thermograms of polymers **I-3** and **I-4**
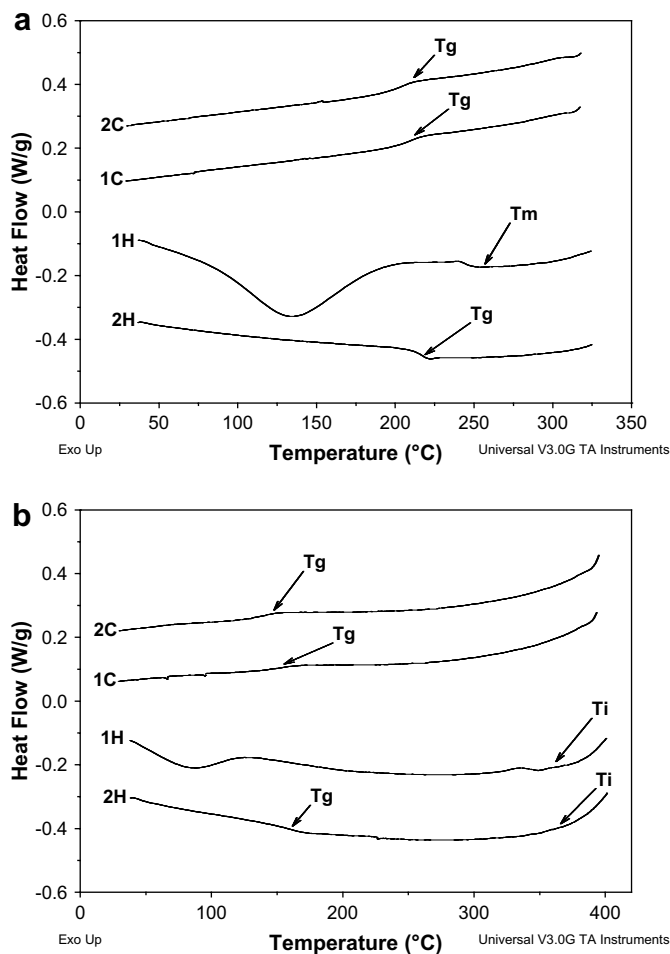
Fig. 1. DSC thermograms of (a) polymer **I-1** and (b) polymer **I-2** obtained at heating and cooling rates of 10 °C/min in nitrogen.

Fig. 2. Photomicrographs of (a) polymer **I-1** taken on annealing at 290 °C overnight and (b) polymer **I-2** taken at 220 °C, respectively, under crossed polarizers exhibiting smectic LC phases (magnification 400×).

were essentially similar in the sense that each of them showed a broad endotherm in the first heating cycle, which was related to the loss of residual solvent in each of these polymers. Each of them showed a single T_g in the second heating cycle. They were at 204 and 107 °C, respectively. In each of the cooling cycles, each of them showed a single T_g, which was slightly lower than that in the second heating cycle. The T_g values for these polymers in the cooling cycles were at 186 and 86 °C, respectively (Fig. S5). The POM studies suggested that they showed weekly birefringence textures recorded at 210 and 195 °C (Fig. S6), which were 5 and 88 °C higher than the corresponding T_g values in the second heating cycles. These weakly birefringent textures are presumably related to the spontaneous alignment promoted by the ionic species present in these polymers that act as a surface treatment agent. This phenomenon is quite common to many ionic LC compounds [10,11]. However, on shearing the viscous melts of these polymers, the development of birefringent textures occurred as observed under the crossed polars suggesting their LC properties (Fig. S6). Note here that the poly-(pyridinium salt)s with $^-BF_4$ as counterions prepared from phenylated bis(pyrylium salt)s and aromatic diamines containing two and three oxyethylene units do not exhibit thermotropic LC properties because of their thermal decomposition prior to melting transitions, although each of them contained more flexible units compared to single oxyethylene unit in the backbone as used in the present study [12]. Therefore, the combination of each of these organic counterions and single oxyethylene unit in each of these ionic polymers is conducive to the formation of thermotropic LC
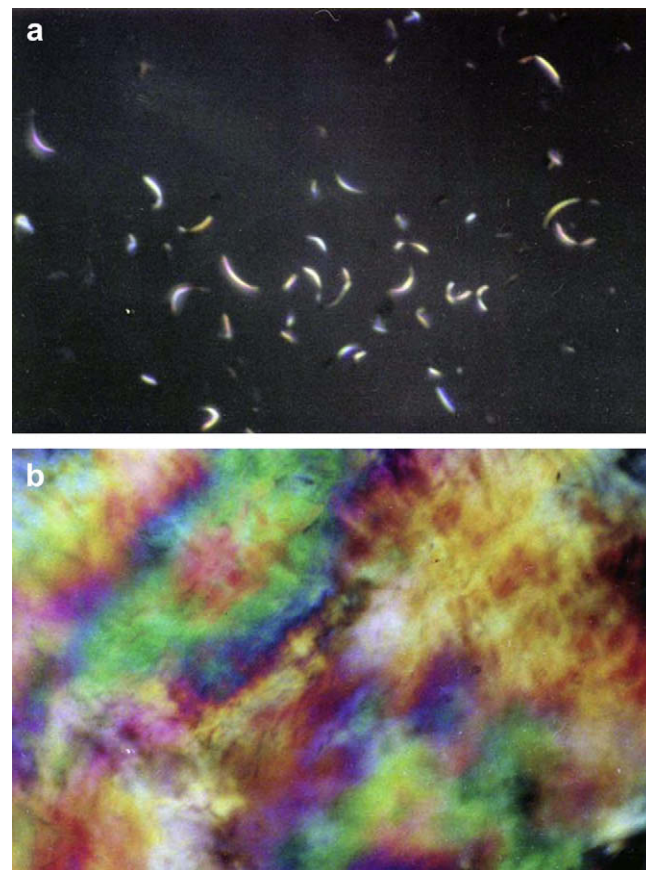
phase without thermal decomposition. The single oxyethylene unit or a multiple thereof as the flexible units either in the main chain or in the side chain were used extensively in the field of thermotropic LC polymers that included polyesters [13–15] and polyimides [8,16–18], among other polymers including ionic polymers [19], to control the thermal transitions of these polymers for LC properties. In recent years, these flexible units were also employed to enhance the solubility of π-conjugated polymers and to fine-tuning their emission of colors for the exploitation of optoelectronic devices.
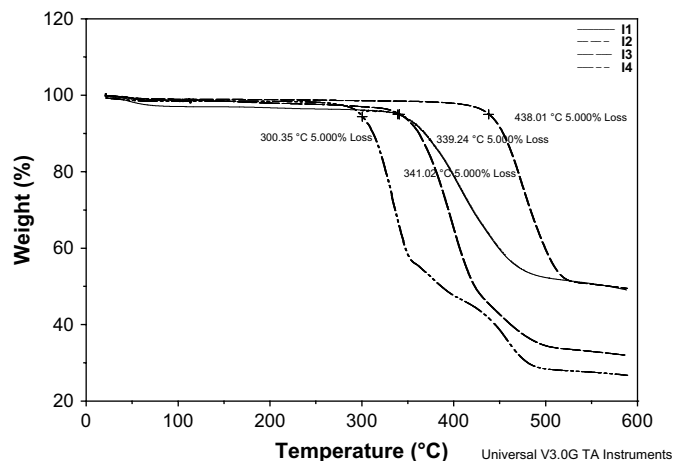

Fig. 3. TGA plots of polymers **I-1**–**I-4** obtained at a heating rate of 10 °C/min in nitrogen.

Additionally, they provide a significant ionic conductivity that can, in principle, be exploited for fabricating light-emitting electrochemical cells [20–24].

3.4. Lyotropic liquid-crystalline properties

The solubility of polymers **I-1**–**I-4** in various polar solvents having dielectric constants within the range of 32.6–48.9 was significant that motivated us to study the lyotropic LC properties in these solvents. Similar to several poly(pyridinium salt)s that exhibit lyotropic LC phase in both protic and aprotic polar solvents [1–4,7], polymer **I-1** containing tosylate as counterion formed an isotropic solution at 10 wt% in methanol ($\varepsilon = 32.6$) at room temperature. At an intermediate concentration (C^*) (20–30 wt%), it formed a biphasic solution wherein there existed an anisotropic (LC phase) and an isotropic phase when examined with a POM under crossed polarizers. At high concentration of 49 wt% in this solvent, it formed a fully-developed lyotropic phase. However, it showed an isotropic phase at high concentration up to 20 wt% in acetonitrile ($\varepsilon = 37.5$), but showed a biphasic solution at its 30 wt% wherein the anisotropic phase could be separable from the isotropic phase on standing at room temperature. It developed fully grown lyotropic phase at 41 wt% in acetonitrile (Fig. 4a). In DMSO ($\varepsilon = 48.9$), it had solubility as high as 49 wt% wherein there was no development of detectable birefringence textures because of high viscosities of these solutions. Polymer **I-2** containing triflimide ion as counterion had very poor solubility in polar protic solvent like methanol at room temperature, but it formed an isotropic solution as high as 20 wt% in acetonitrile. At high concentration of 40 wt% in this solvent, there was a development of weak birefringent texture, however, because of high viscosity at still higher concentration solution of this polymer precluded the development of fully grown lyotropic phase. Its solution properties in DMSO were essentially identical to those in acetonitrile. Polymer **I-3** containing DBS as counterion formed isotropic solution as high as at 20 wt% in methanol, biphasic solution at 30 wt% and lyotropic phase 39 wt% in methanol. Similarly, its C^* and concentration for the formation of biphasic solution and lyotropic phase were 10 and 39 wt% in acetonitrile, respectively. Like polymer **I-1**, polymer **I-3** also had solubility as high as 30 wt% in DMSO, but these solutions did not develop any detectable birefringence textures because of high viscosity of these solutions, which precluded establishing their lyotropic LC properties. Polymer **I-4** containing docusate as counterion formed an isotropic solution at 20 wt% in methanol. Its C^* and concentration for the formation of biphasic solution and lyotropic phase (Fig. 4b) were 30 and 41 wt%, respectively, in this solvent. In acetonitrile, its C^* (10 wt%) was at lower concentration than that in methanol, but the concentration for the formation of lyotropic phase was essentially identical. In DMSO, it formed an isotropic solution at a concentration up to 30 wt%; and its biphasic solution appeared at 40 wt% in this solvent. However, like polymer **I-2**, its fully grown lyotropic phase could not be determined because of high viscosity at still higher concentration of polymer **I-4** in this solvent. Note here that the difficulty in the preparation of thin films from highly viscous solutions of ionic polymers hindered the development LC textures, since the well-developed textures in LC polymers usually occur in thin films under crossed polarizers [7]. Their high solubility in various polar solvents was related to the high solvophilic effects of these solvents with the pyridinium ions associated with various organic counterions in conjunction with single oxyethylene unit present along the backbones of these polymers.

3.5. Photoluminescence properties

Since each of the ionic polymers **I-1**–**I-4** contained organic counterions, which were associated with phenylated pyridinium
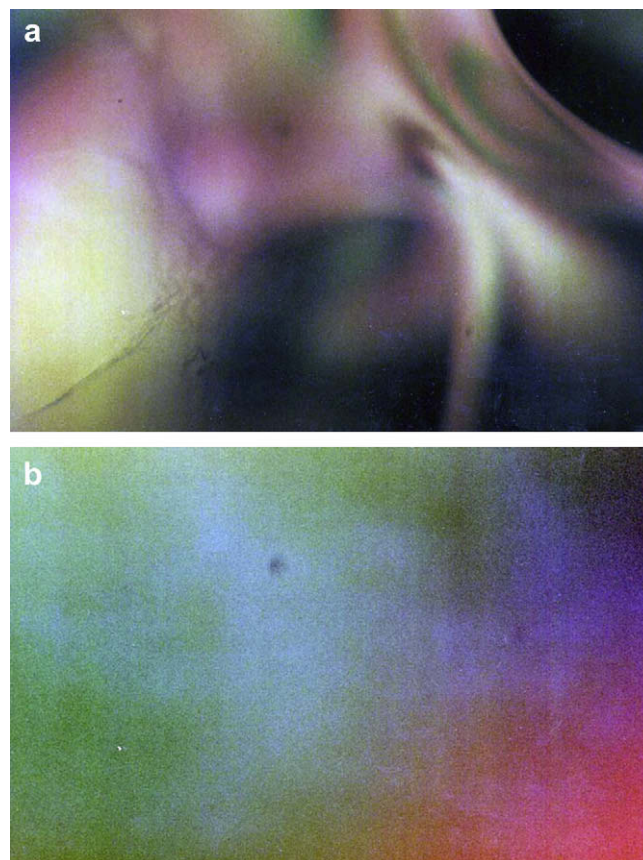

Fig. 4. Photomicrographs of: (a) polymer **I-1** at 41 wt% in CH$_3$CN and (b) polymer **I-4** at 41 wt% in methanol under crossed polarizers exhibiting lyotropic LC phases, respectively (magnification 400×).

moieties, and single oxyethylene unit in their backbones, they had good solubility in various polar organic solvents. Polymer **I-2** containing triflimide as counterion had also sufficient solubility in low polar solvent such as acetone, but very low solubility in protic polar solvent such as methanol at room temperature (*vide supra*). Their solubility in various organic solvents allowed us to measure the optical properties that included UV–vis absorption spectra and photoluminescence properties in their solutions as well as in their thin-film states cast from various solvents. For example, polymer **I-2** showed a λ_{max} at 330, 335 and 340 nm in acetone, acetonitrile and DMSO, respectively. The bathochromic shift in its λ_{max} values with the increase in relatively low polar solvent to high polar solvent suggested that all of these absorption maxima were indicative of closely spaced π–π^* transitions common to aromatic rings. A model compound what is known as 1,2,4,6-tetraphenylpyridinium perchlorate exhibits essentially an identical absorption spectrum with a $\lambda_{max} = 312$ nm in ethanol. The absorption band of *ortho*-substituted pyridinium salt consists of two electronic transitions that are intramolecular charge transfer complexes of the 2,6- and the 4-substituent with the positively charged nitrogen center [25]. Thus, it was reasonable to state that the absorption bands for all these polymers arose from the identical electronic transitions as those in closely related pyridinium salts. The optical band gaps of polymer **I-2**, that is, E_g values as determined from the onset of wavelength in the UV–vis spectra in acetone, acetonitrile and DMSO were 3.35, 3.02 and 2.97 eV. These E_g values were higher than those of a class of π-conjugated light-emitting polymers including poly(*p*-phenylenevinylene)s [26,27], but comparable with those of other related poly(pyridinium salt)s [6,28].
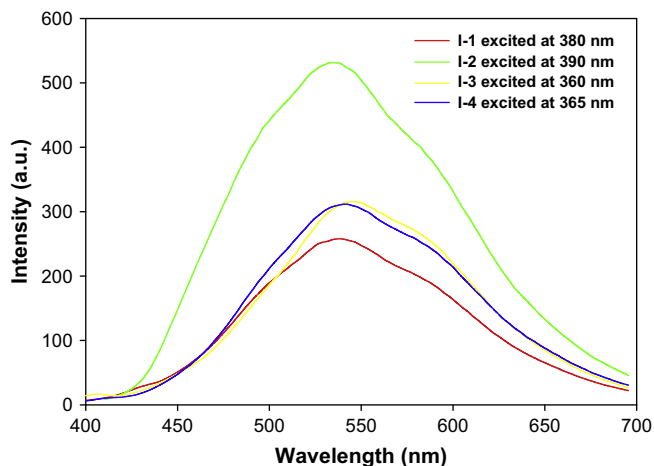
Fig. 5. Emission spectra of polymers **I-1**–**I-4** in acetonitrile at various excitation wavelengths.

Fig. 6. Emission spectra at various excitation wavelengths and excitation spectrum monitored at 540 nm of polymer **I-2** in dimethyl sulfoxide.

Fig. 5 shows the photoluminescence spectra of polymers **I-1**–**I-4** in acetonitrile at various excitation wavelengths. Each of the emission spectra showed a distinct, broad λ_{em} peak without discernible vibrational fine structures. Note here that the appearance of broad structureless band of polymer is usually associated with intramolecular processes, more exactly, with the strong interaction of vibrations rather than intermolecular processes. This interaction makes impossible the localization of energy at certain vibrational degree of freedom, that is, on excitation of a vibration by light, the respective energy is redistributed very fast around the entire system of vibration levels. The full width at half-maximum (fwhm) value for each of the emission spectrum is quite broad. However, the fwhm value was the highest for polymer **I-4** and that was the lowest for polymer **I-1** in this solvent. Their λ_{em} peaks were slightly dependent on the nature of counterions in an aprotic polar solvent like acetonitrile. Polymers **I-2** and **I-4** had essentially an identical λ_{em} peak at ca. 533 nm; and polymers **I-1** and **I-3** had essentially an identical λ_{em} peak at ca. 541 nm in their emission spectra. Therefore, polymers **I-1** and **I-3** showed a bathochromic shift of 8 nm in their emission spectra in this polar solvent when compared with those of polymers **I-2** and **I-4**. However, their excitation spectra consisted of two major λ_{ex} peaks at ca. 262 and 382 nm along with several vibrational fine structures when monitored at ca. 545 nm wavelength of light (not shown). In methanol, polymers **I-1**, **I-3** and **I-4** showed λ_{em} peak at 532, 537 (two shoulder peaks 579 and 607) and 537 nm when excited at various excitation wavelengths of 265, 360 and 385 nm light. Their excitations spectra in this solvent were essentially very similar to those in acetonitrile. In DMSO, polymer **I-1** solution showed a λ_{em} peak at ca. 540 nm when excited at 265, 395 and 405 nm wavelengths of light, albeit it required a relatively high concentration of this polymer for the measurement of light emission in this solvent. Its λ_{em} peak was independent of the excitation wavelengths of light used. Its excitation spectrum showed two λ_{ex} peaks at 264 and 393 nm when monitored at 540 nm wavelength of light. In contrast, polymer **I-2** showed various λ_{em} peaks that ranged from 544 to 592 nm in this solvent depending on the excitation wavelengths used (Fig. 6). Unlike polymer **I-1**, it showed a single a λ_{ex} peak at 427 nm when monitored at 540 nm wavelength of light. Both the excitation and emission spectra of polymer **I-3** in this solvent were essentially similar to those in polymer **I-1**, except that its λ_{em} peak was slightly shifted hypsochromically to 536 nm at identical excitation wavelength. It also required a relatively high concentration of this polymer solution for the measurement of emission of light.
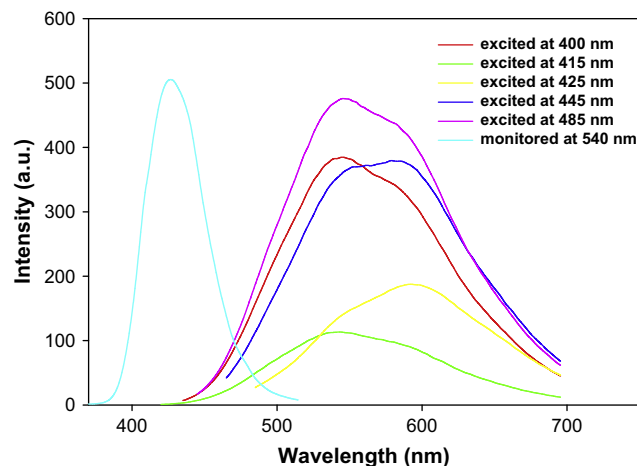
Polymer **I-4** showed a single λ_{ex} peak at 410 nm when monitored at 540 nm wavelength of light, like polymer **I-2**. In its emission spectrum, there was a single λ_{em} peak at 542 nm, which was slightly shifted bathochromically when compared with those of polymers **I-1** and **I-3**. In acetone ($\varepsilon = 20.6$), polymer **I-2** showed a λ_{em} peak at ca. 540 nm when excited at 395 and 405 nm. However, its fwhm value was much narrower than those in other solvents (Fig. S7). There was a single λ_{ex} peak at 394 nm when monitored at 540 nm wavelength of light.

The films of polymers **I-1**–**I-4** were prepared from their respective solutions (methanol or acetonitrile) casting onto quartz plates. In the case of polymer **I-2**, thin film was cast from hot methanol solution, because of very low solubility of this polymer in this solvent at room temperature. The solid-state emission spectra of polymers **I-1**–**I-4** cast from two different solvents are shown in Fig. 7. In thin films when cast from methanol solutions, all of these polymers showed a major λ_{em} peak in their emission spectra with the complete loss of vibrational fine structures at 496, 487, 497, and 480 nm, respectively, when excited at 340, 330, 340 and 340 nm wavelengths of light (Fig. 7a). Their excitation spectra showed a single λ_{ex} peak in the broad range of 325–338 nm when monitored at the wavelengths of their λ_{em} peak values. On changing from solutions to the thin films, polymers **I-1**, **I-3**, and **I-4** showed large hypsochromic shifts of 36, 40, and 57 nm in their λ_{em} values, when compared with those of solution spectra. Similarly, when their films were cast from another solvent acetonitrile, they also showed a major λ_{em} peak in their emission spectra with the complete loss of vibrational fine structures at 503, 495, 489, and 488 nm when excited at 340, 330, 340 and 340 nm wavelengths of light (Fig. 7b). Polymer **I-1** showed several λ_{ex} peak values at 308, 337, 286, and 439 when monitored at 500 nm. In contrast, polymer **I-2** and **I-3** showed a single λ_{ex} peak when monitored at 495 and 490 nm wavelengths of light. Polymer **I-4** had two λ_{ex} peak values at 329 and 393 when monitored at 485 nm. On changing from solutions to the thin films, they showed large hypsochromic shifts of 38, 38, 52, and 45 nm in their λ_{em} values, when compared with those of solution spectra. The fwhm values of emission spectra in thin films of these polymers cast from both methanol and acetonitrile were relatively narrower when compared with those in their solutions spectra in these solvents. These features strongly suggest that there existed less ordered structures in the solid-state morphology of these ionic polymers. Note here that both intra- and intermolecular π–π interactions of chromophores of polymers are mainly responsible for the ordered structures, which in turn usually cause
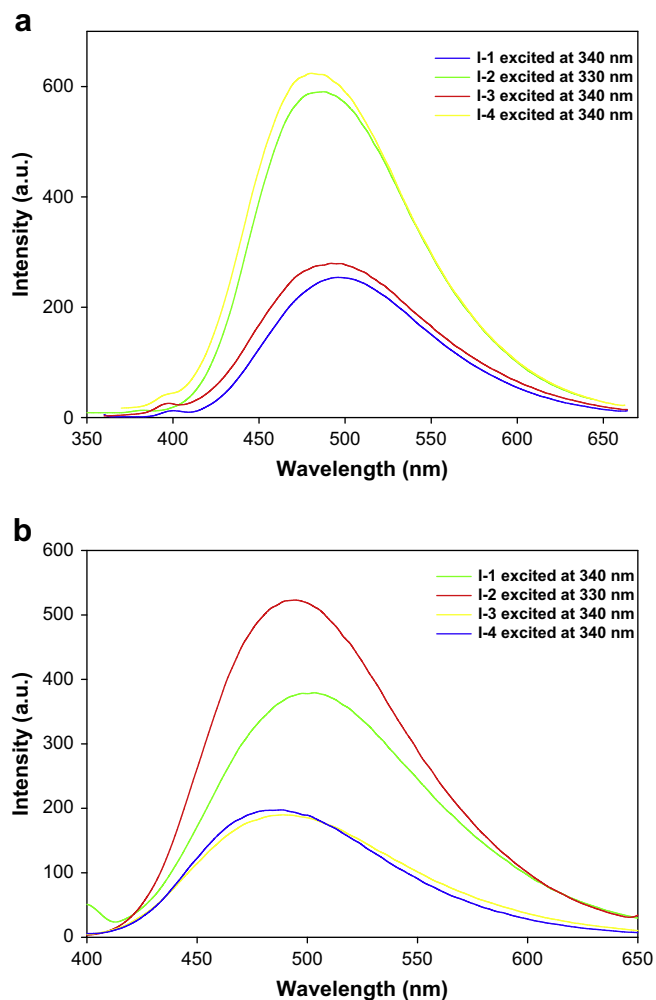
Fig. 7. Emission spectra of polymers **I-1**–**I-4** in thin films at various excitation wavelengths: (a) cast from methanol and (b) cast from acetonitrile, respectively.

both to shift λ_{em} bathochromically to a great extent as high as 100 nm or higher and to lower the quantum yields of light-emitting polymers in the solid state in general [29,30]. These π–π interactions of chromophores were essentially minima in this class of poly(pyridinium salt)s containing oxyethylene unit. The light emission for each of these polymers occurred in the solid state in the blue region of the visible light.

4. Conclusions

Several poly(pyridinium salt)s with organic counterions (OTs, NTf$_2$, DBS, and docusate) were prepared by either the ring-transmutation polymerization of phenylated bis(pyrylium tosylate) salt with 1,2-bis(4-aminophenoxy)ethane in DMSO or the metathesis reaction of the tosylate polymer with the corresponding lithium or sodium salts in acetonitrile. Their chemical structures were determined by spectroscopic techniques and elemental analysis. Their intrinsic viscosities and weight-average molecular weights were in the range of 0.59–1.22 dL/g and 83,000–105,000, respectively, as determined by GPC. They were characterized for their both thermotropic and lyotropic liquid-crystalline properties with various experimental techniques. For example, polymer **I-1** with tosylate as counterion exhibited smectic liquid-crystalline phase at low temperature that persisted up to its decomposition temperature. The corresponding polymer **I-2** with triflimide as counterions had

not only low T_m value but also low T_i value thus exhibiting a broad temperature range of LC phase. It had also the highest thermal stability in the series of these ionic polymers. Additionally, polymer **I-1** at 41 wt% in acetonitrile and polymer **I-4** at 41 wt% in methanol displayed lyotropic LC phase. They are the novel members of a class of poly(pyridinium salt)s that exhibited both lyotropic and thermotropic liquid-crystalline properties, which can be classified as amphotropic polymers. Although the literature is replete with many lyotropic (solvent induced) and many thermotropic (heat induced) liquid-crystalline polymers [31], relatively few amphotropic liquid-crystalline polymers both neutral and ionic polymers exist to date [7,32–36].

All of them exhibited light-emitting properties both in polar organic solvents as well as in the solid state. For example, polymer **I-1** emitted light of wavelengths 532 nm in methanol and 541 nm in acetonitrile solutions. In its thin films cast from both methanol and acetonitrile, the wavelengths of light emission were shifted hypsochromically to 496 and 503 nm, respectively, because of the less ordered structures in the solid state.

The combination of thermotropic and lyotropic liquid-crystalline properties, the ease of film formation, and photoluminescence makes these polymers interesting for optoelectronic applications such as polymer light-emitting devices, especially light-emitting electrochemical cells. They are also ideal cationic polymers for the preparation of multilayer assemblies with controlled morphologies at a molecular level by the sequential deposition technique with anionic polymers.

Acknowledgments

Appendix. Supplementary data

Supplementary data associated with this article can be found in the online version, at doi:10.1016/j.polymer.2009.05.010.

References

[1] Bhowmik PK, Burchett RA, Han H, Cebe JJ. Macromolecules 2001;34:7579.
[2] Bhowmik PK, Han H, Nedeltchev AK. Polymer 2006;47:8281.
[3] Bhowmik PK, Burchett RA, Han H, Cebe JJ. J Polym Sci Part A Polym Chem 2001;39:2710.
[4] Bhowmik PK, Burchett RA, Han H, Cebe JJ. Polymer 2002;43:1953.
[5] Bhowmik PK, Han H, Cebe JJ, Nedeltchev IK, Kang S-W, Kumar S. Macromolecules 2004;37:2688.
[6] Bhowmik PK, Han H, Nedeltchev AK. J Polym Sci Part A Polym Chem 2006;44:1028.
[7] Bhowmik PK, Kamatam S, Han H, Nedeltchev AK. Polymer 2008;49:1748.
[8] Feld WA, Ramalingam B, Harris FW. J Polym Sci Polym Chem Ed 1983;21:319.
[9] Katritzky AR, Brownlee RTC, Musumarra G. Tetrahedron 1980;36:1643.
[10] Binnemans K. Chem Rev 2005;105:4148.
[11] Godinho MH, Cruz C, Teixeira PIC, Ferreira AJ, Costa C, Kulkarni PS, et al. Liq Cryst 2008;35:103.
[12] Harris FW, Chuang KC, Huang SAX, Janimak JJ, Cheng SZD. Polymer 1994;35:4940.
[13] Ober C, Lenz RW, Galli G, Chiellini E. Macromolecules 1983;16:1034.
[14] Bhowmik PK, Garay RO, Lenz RW. Makromol Chem 1991;192:415.
[15] Lenz RW, Furukawa A, Bhowmik PK, Garay RO, Majnusz J. Polymer 1991;32:1703.
[16] Kricheldorf HR. Adv Polym Sci 1999;141:83.

[17] Eastmond GC, Paprotny J. Polymer 2002;43:3455.
[18] Costa G, Eastmond GC, Fairclough JPA, Paprotny J, Ryan AJ, Stagnaro P. Macromolecules 2008;41:1034.
[19] Han H, Vantine PR, Nedeltchev AK, Bhowmik PK. J Polym Sci Part A Polym Chem 2006;44:1541.
[20] Pei Q, Yang Y. J Am Chem Soc 1996;118:7416.
[21] Yang C, He G, Wang R, Li Y. Mol Cryst Liq Cryst 1999;337:473.
[22] Cacialli F, Friend RH, Feast WJ, Lovenich PW. Chem Commun 2001:1778.
[23] Mihara T, Yada T, Koide N. Mol Cryst Liq Cryst 2004;411:421.
[24] Hargadon MT, Davey EA, McIntyre TB, Gnanamgari D, Wynne CM, Swift RC, et al. Macromolecules 2008;41:741.
[25] Makoswski MP, Mattice WL. Polymer 1993;34:1606.
[26] Kraft A, Grimsdale AC, Holmes AB. Angew Chem Int Ed 1998;37:402.
[27] Mitschke U, Bäuerle P. J Mater Chem 2000;10:1471.

[28] Spiliopoulos IK, Mikroyannidis JA. J Polym Sci Part A Polym Chem 2001; 39:2454.
[29] Sarker AM, Strehmel B, Neckers DC. Macromolecules 1999;32:7409.
[30] Gettinger C, Heeger AJ, Drake J, Pine D. J Chem Phys 1994;101:1673.
[31] Donald AM, Windle AH. Liquid crystalline polymers. Cambridge: Cambridge University; 1999. p. 1–310.
[32] Aharoni SM. J Polym Sci Polym Phys Ed 1980;18:1303.
[33] Kaeriyama K, Kouyama S, Sekita M, Nakayama T, Tsukahara Y. Macromol Rapid Commun 1999;20:50.
[34] Bhowmik PK, Han H, Nedeltchev IK. J Polym Sci Part A Polym Chem 2002; 40:2015.
[35] Mruk R, Prehl S, Zentel R. Macromol Chem Phys 2004;205:2169.
[36] Choi K, Mruk R, Moussa A, Jonas AM, Zentel R. Macromolecules 2005;38: 9124.